

physiological emphasis); (3) Sections 8.3 and 8.7 (population biology); (4) Sections 8.3, 8.4, 8.6, and 8.8 (mathematical techniques with examples drawn from molecular models).

CONDUCTION, THE ACTION POTENTIAL, HODGKIN-HUXLEY EQUATIONS

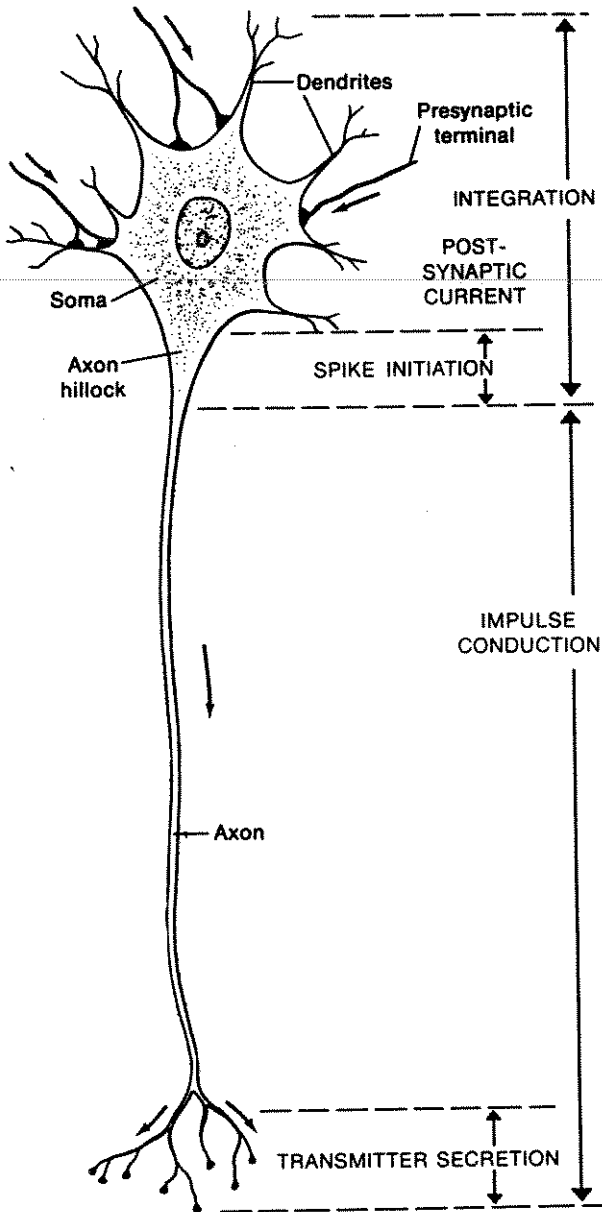
One of the leading frontiers of biophysics is the study of neurophysiology, which only several decades ago spawned an understanding of the basic processes underlying the unique electrochemical communication system that constitutes our nervous system. Our brains and every other subsystem in the nervous system are composed of cells called *neurons*. While these vary greatly in size, shape, and properties, such cells commonly share certain typical features (see Figure 8.2). Anatomically, the cell body (*soma*) is the site at which the nucleus and major subcellular structures are located and is the central point from which synthesis and metabolism are coordinated.

A more prominent feature is a long tube-like structure called the *axon* whose length can exceed 1 meter (that is, $\sim 10^5$ times the dimension of the cell body). It is known that the propagation of a nerve signal is electrical in nature; after being initiated at a site called the *axon hillock* (see Figure 8.2) propagates down the length of the axon to terminal branches, which form loose connections (*synapses*) with neighboring neurons. A propagated signal is called an *action potential* (see Figure 8.3).

A neuron has a collection of *dendrites* (branched, "root-like" appendages), which receive incoming signals by way of the synapses and convey them to the soma.

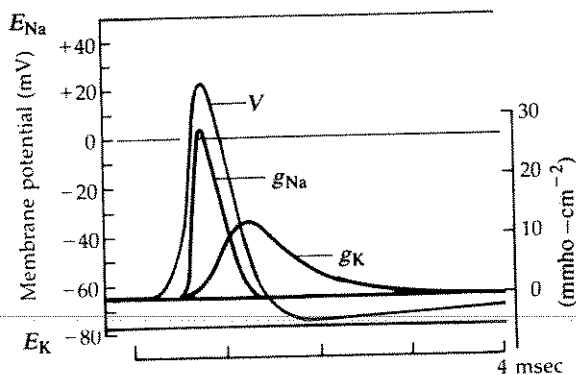
How the detailed electrochemical mechanism operates is a fascinating story that, broadly speaking, is now well understood. It is known that neuronal signals travel *along the cell membrane* of the axon in the form of a local voltage difference across the membrane. A word of explanation is necessary. In the *resting state* the cytoplasm (cellular fluid) inside the axon contains an ionic composition that makes the cell interior slightly negative in potential (-50 mV difference) with respect to the outside (see Figure 8.4). Such a potential difference is maintained at a metabolic expense to the cell by *active pumps* located on the membrane. These continually transport sodium ions (Na^+) to the outside of the cell and convey potassium ions (K^+) inwards so that concentration gradients in both species are maintained. The differences in these and other ionic concentrations across the membrane result in the net electric potential that is maintained across the membrane of the living cell. In this section we take the convention that the voltage v is the potential difference (inside minus outside) for the membrane.

Thinking of the axon as a long electrical cable is a vivid but somewhat erroneous conception of its electrical properties. First, while a current is implicated, it is predominantly made up of ionic flow (not electrons), and its direction is not longitudinal but transverse (into the cell) as shown in Figure 8.5. Second, while a passive cable has fixed resistance per unit length, an axon has an *excitable membrane* whose resistance to the penetration of ions changes as the potential difference v is raised.



atic representation of a neuron
ody (soma) which receives stimuli
he axon along which impulses
d the terminal branches that form

connections (synapses) with other neurons. [From
Eckert, R., and Randall, D. *Animal Physiology*, 2d
edition. W. H. Freeman and Company. Copyright
© 1983, p. 179.]

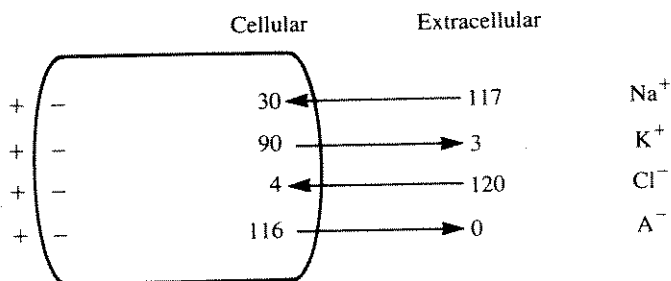


action potential consists of local change across the axon membrane y changes in the conductivities of the Na^+ and K^+ (g_{Na} , g_{K}) in a time t here. (Note: mho, a unit commonly used here, is equivalent to $1/\text{ohm}$.) This

signal is generally propagated along the neuronal axon from soma to terminal branches. [After Hodgkin and Huxley (1952), from Kuffler, Nicholls, and Martin (1984) p. 151, fig. 13A, From Neuron to Brain, 2nd edition, by permission of Sinauer Associates Inc.]

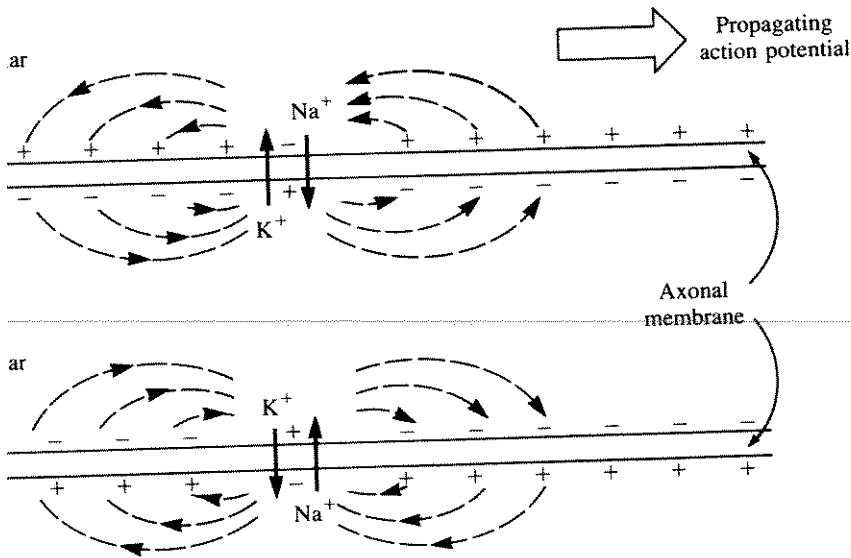
The flow of charged ions across a cell membrane is restricted to specific molecular sites called *pores*, which are sprinkled liberally along the membrane surface. It is now known that many different kinds of pores (each specific to a given ion) are present and that these open and close in response to local conditions including the electrical potential across the membrane. This can be broadly understood in terms of changes in the conformation of the proteins making up these pores, although the biophysical details are not entirely known.

To understand the process by which an action potential signal is propagated, we must look closely at events happening in the immediate vicinity of the membrane. Starting the process requires a *threshold voltage*: the potential difference must be raised to about -30 to -20 mV at some site on the membrane. Experimentally



the resting state, cells have an ionic concentration (given here in millimolar units) that is different from that of their environment. Active transport maintains a lower sodium (Na^+) and a

higher potassium (K^+) concentration inside the cell. Cl^- and A^- represent respectively chlorine ions and other ionic species such as proteins.



When the axon of a neuron receives a stimulus at some point along its length, the activities of the membrane for Na^+ and K^+ ions permit them to cross the

axonal membrane, creating local currents. Since adjacent portions of the membrane are thereby stimulated, the wave of activity known as the action potential can be propagated.

As an action potential can be done by a stimulating electrode that pierces a single neuron. Biologically, this happens at the axon hillock in response to an integrated appraisal of excitatory inputs impinging on the soma. As a result of reaching this threshold voltage, the following sequence of events occurs (see Figure 8.6):

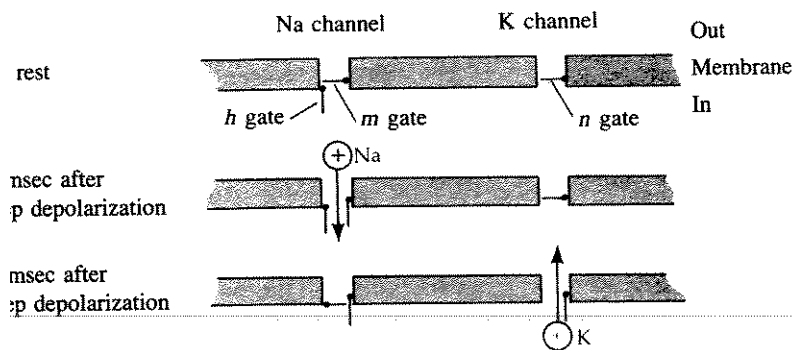
Sodium channels open, letting a flood of Na^+ ions enter the cell interior. This causes the membrane potential to *depolarize* further; that is, the inside becomes positive with respect to the outside, the reverse of resting-state polarization.

After a slight delay, the potassium channels open, letting K^+ leave the cell. This restores the original polarization of the membrane, and further causes an overshoot of the negative rest potential.

The sodium channels then close in response to a decrease in the potential difference.

Adjacent to a site that has experienced these events the potential difference exceeds the threshold level necessary to set in motion step 1. The process repeats, leading to spatial conduction of the spike-like signal. The action potential can thus be transported down the length of the axon without attenuation or change in shape. Mathematically, this makes it a *traveling wave*.

The finer details of this somewhat impressionistic description were uncovered in 1952 in a series of brilliant but painstaking experiments due to Hodgkin, Huxley, and Katz on the giant squid axon, a cell whose axonal diameter is large enough to



Typical time sequence depicting the action potential in an axon. Shown are separate pores, h , m , and n , for the ions Na^+ and K^+ . At rest all gates are closed. When a threshold is reached, the m gates open rapidly,

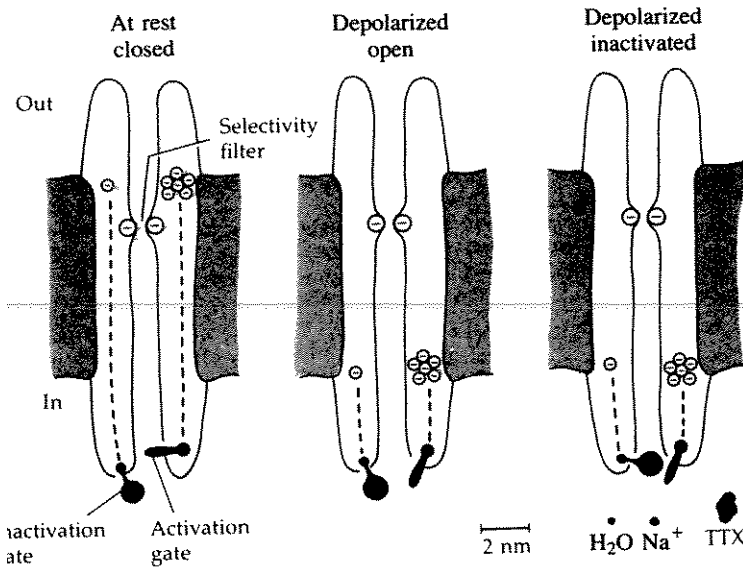
followed by changes in the other gates. [From Kuffler, Nicholls, and Martin (1984), p. 149, fig. 12. From *Neuron to Brain*, 2nd edition, by permission of Sinauer Associates Inc.]

Permit intracellular recording of the voltage by microelectrodes. One technique particularly useful in elucidating the time sequence of ionic conductivities is the *voltage-clamp* experiments. In these, an axon is excised from its cell and its contents are emptied (in a manner akin to squeezing a tube of toothpaste). A thin wire inserted into the hollow axon replaces its cytoplasm and permits an artificially constant voltage to be applied simultaneously along its length. Provided the preparation is kept physiologically active, one can observe a spatially constant but time-varying voltage across the membrane. This voltage has typical action-potential characteristics.

It is further possible to follow the time behavior of the ionic conductivities by a variety of techniques. These include *patch-clamp* experiments, in which single pores are isolated on bits of membrane by suction using fine micropipettes or by selective ionic blocking using agents, such as tetrodotoxin, that bind to ionic pores in a specific way. The detailed structure of some ionic pores is beginning to emerge by a combination of techniques including electron microscopy. (See Figure 8.7.)

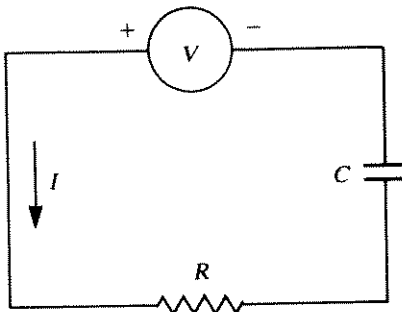
With this physiological description we can now discuss the mathematical model that has played a significant role in the advances in neurophysiology. First, a brief review of terminology and properties of an electrical circuit is provided in the next section.

The example given in the box, when somewhat modified, can be used to depict the electrical properties of the axonal membrane. The idea underlying the approach on which the Hodgkin-Huxley model is based is to use an electric-circuit analog in which physical properties such as ionic conductivities are represented as circuit elements (resistors). The voltage across the membrane thus corresponds to voltage across a collection of resistors, each one depicting a set of ionic pores that selectively permit a limited current of ions. By previous discussions, the resistance (or equivalently, the *conductivities* of such pores) depends on voltage.

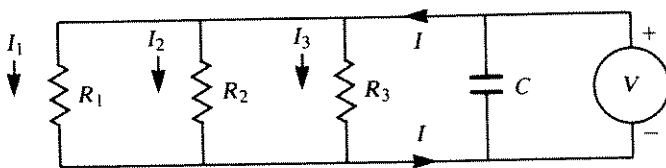


biochemical, electron microphysiological information shown are the activation gates and permits selectivity to Na⁺. Also

shown to scale are molecules of water, sodium, and the blocking agent tetrodotoxin (TTX). [From Kuffler, Nicholls, and Martin (1984), p. 156, fig. 15. From Neuron to Brain, 2nd edition, by permission of Sinauer Associates Inc.]



(a)



(b)

multiple electric circuit. (b) Circuit showing several elements in parallel.

Electric Circuit

The following terms are applied in describing a circuit, such as the one shown in Figure 8.8(a).

- $q(t)$ = the charge (net positive or negative charge carried by particles in the circuit at time t),
- $I(t)$ = the current (rate of flow of charge in the circuit) = dq/dt ,
- $V(t)$ = the voltage (electromotive force that causes motion of charge; also a measure of the difference in the electrical potential across a given element or set of elements),
- R = resistance (property of a material that tends to impede the flow of charged particles),
- g = conductance = $1/R$,
- C = capacitance (a property of any element that tends to separate physically one group of charged particles from another; this causes a difference in electric potential across the element, called a capacitor).

The following physical relationships hold in a circuit:

1. *Ohm's law*: the voltage drop across a resistor is proportional to the current through the resistor; R or $1/g$ is the factor of proportionality:

$$V_R(t) = I(t)R = \frac{I(t)}{g}. \tag{2}$$

2. *Faraday's law*: the voltage drop across a capacitor is proportional to the electric charge; $1/C$ is the factor of proportionality:

$$V_C(t) = \frac{q(t)}{C}. \tag{3}$$

3. *Kirchhoff's law*: the voltage supplied is equal to the total voltage drops in the circuit. For example:

$$V(t) = V_R(t) + V_C(t).$$

4. For several elements in parallel, the total current is equal to the sum of currents in each branch; the voltage across each branch is then the same. In the example shown in Figure 8.8(b) the current is

$$\begin{aligned} I(t) &= I_1(t) + I_2(t) + I_3(t) = \frac{V}{R_1} + \frac{V}{R_2} + \frac{V}{R_3} \\ &= V(g_1 + g_2 + g_3). \end{aligned} \tag{4a}$$

Also,

$$V(t) = q(t)C. \tag{4b}$$

Differentiating (4b) leads to

$$\frac{dV}{dt} = \frac{1}{C} \frac{dq}{dt} = \frac{I(t)}{C}. \tag{4c}$$

Thus

$$\frac{dV}{dt} = \frac{V(t)}{C} (g_1 + g_2 + g_3). \quad (4d)$$

In the circuit analog of an axon shown in Figure 8.9, resistance to ionic flow across the membrane is depicted by the conductivities g_K , g_{Na} , and g_L . Resistance to ionic motion inside the axon in an axial direction is represented by longitudinal elements whose resistance per unit length is fixed and much higher than that of the medium surrounding the outer membrane. (The axon has a small radius, which implies greater resistance to flow.) The finite thickness of the membrane is associated with its property of *capacitance*, that is, a separation of charge. We must remember, looking at this schematic representation, that the axon is cylindrical. Therefore the following modified definitions prove convenient:

- $q(x, t)$ = charge density inside the axon at location x and time t (units of charge per unit length),
 C = capacitance of the membrane per unit area,
 a = radius of the axon,
 $I_i(x, t)$ = net rate of exit of positive ions from the exterior to the interior of the axon per unit membrane area at (x, t) ,
 $v(x, t)$ = departure from the resting voltage of the membrane at (x, t) .

Then by previous remarks the following relationship is satisfied:

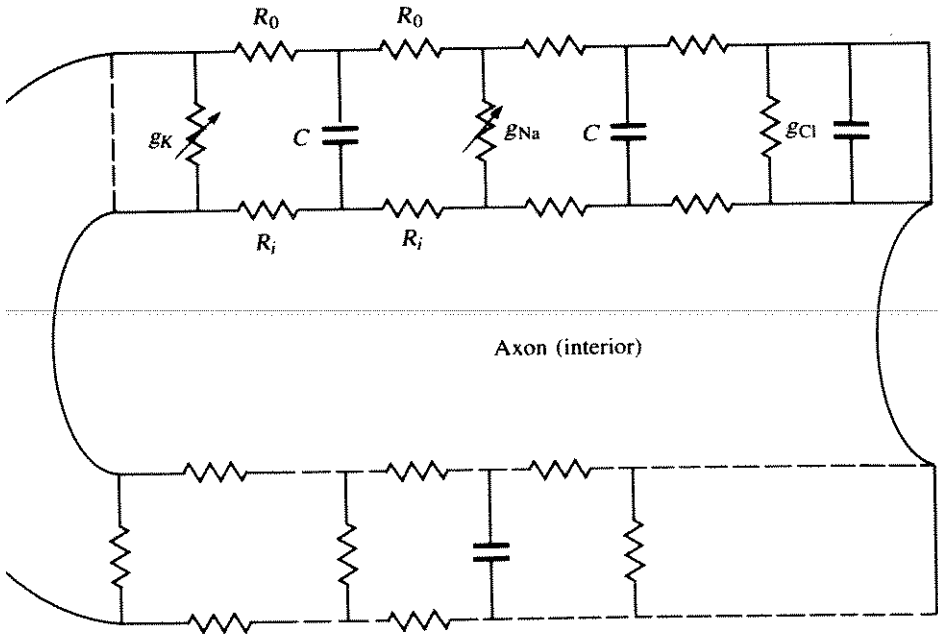
$$q(x, t) = 2\pi a C v(x, t). \quad (5)$$

We shall now assume that a voltage clamp is applied to the axon so that $v = v(t)$ and thus all points on the inside of the axon are at the same voltage at any instant. This means that charge will not move longitudinally (there is no force leading to its motion). It can only change by currents that convey ions across the cell membrane. In this case the rate of change of internal charge can be written

$$\frac{dq}{dt} = -2\pi a I_i. \quad (6)$$

The current I_i can be further expressed as a sum of the three currents I_{Na} , I_K , and I_L (sodium, potassium, and all other ions) and related to the potential difference that causes these, as follows:

$$\frac{dq}{dt} = -2\pi a (I_{Na} + I_K + I_L), \quad (7)$$



schematic version of the electric m roughly equivalent to the axonal c , g_{Na} , and g_{Cl} are the voltage-conductivities to K^+ , Na^+ , and Cl^- ; R_i

and R_0 represent the resistance of inside and outside environments; C depicts the membrane capacitance. (Note: g_{Cl} is assumed to be constant.)

$$I_{Na} = g_{Na}(v - v_{Na}), \quad (8a)$$

$$I_K = g_K(v - v_K), \quad (8b)$$

$$I_L = g_L(v - v_L). \quad (8c)$$

Here v_{Na} , v_K , and v_L represent that part of the resting membrane potential that is due to the contributions of the ions Na^+ , K^+ , and L (all other mobile species). Furthermore, equation (7) in its entirety may be written in terms of voltage by using equation (5), with the result that

$$\frac{dv}{dt} = -\frac{1}{C}[g_{Na}(v)(v - v_{Na}) + g_K(v)(v - v_K) + g_L(v - v_L)]. \quad (9)$$

It is generally assumed that g_L is independent of v (is constant). At this point Hodgkin, Huxley, and Katz departed somewhat from a straightforward electrical analysis and went on to speculate on a possible mechanism governing the ionic conductivities g_{Na} and g_K . After numerous trial-and-error models, laboriously solved on mechanical calculators, they found it necessary to introduce three variables n , m , and h in the dynamics of the ionic pores. These hypothetical quantities could perhaps be interpreted as concentrations of proteins that must act in concert to open or close a pore. (See Figure 8.6.) However, the equations were chosen to fit the data, not from a more fundamental knowledge of molecular mechanisms.

They defined

$$g_{Na} = \bar{g}_{Na} m^3 h, \tag{10}$$

$$g_K = \bar{g}_K n^4, \tag{11}$$

where \bar{g} 's are constant conductivity parameters. They suggested that n , m , and h are voltage-sensitive gate proteins (see Figures 8.6 and 8.7), that obey differential equations in which voltage dependence is described:

$$\frac{dn}{dt} = \alpha_n(v)(1 - n) - \beta_n(v)n, \tag{12a}$$

$$\frac{dm}{dt} = \alpha_m(v)(1 - m) - \beta_m(v)m, \tag{12b}$$

$$\frac{dh}{dt} = \alpha_h(v)(1 - h) - \beta_h(v)h. \tag{12c}$$

In addition, the quantities α_n , α_m , α_h , β_n , β_m , and β_h are assumed to be voltage-dependent as follows:

$$\alpha_n(v) = 0.1(v + 25)(e^{(v+25)/10} - 1)^{-1}, \quad \beta_m(v) = 4 e^{v/18}, \tag{13a,b}$$

$$\alpha_h(v) = 0.07 e^{v/20}, \quad \beta_h(v) = (e^{(v+30)/10} + 1)^{-1}, \tag{13c,d}$$

$$\alpha_m(v) = 0.01(v + 10)(e^{(v+10)/10} - 1)^{-1}, \quad \beta_n(v) = 0.125 e^{v/80}. \tag{13e,f}$$

The values of other constants appearing in the equations are $\bar{g}_{Na} = 120$, $\bar{g}_K = 36$, and $g_L = 0.3 \text{ mmho cm}^{-2}$; $v_{Na} = -115$, $v_K = 12$, and $v_L = -10.5989 \text{ mV}$.

With a physiological system as intricate as the neural axon, it is reasonable to expect rather complicated interactions between variables. In assessing the Hodgkin-Huxley model, we should keep in mind that all but one of its equations were tailored to fit experimental observations. Part of the surprisingly great success of the model lies in its ability to predict fairly accurately the results of many other observations not used in formulating the equations. A valid criticism of the model is that the internal variables m , n , and h do not clearly relate to underlying molecular mechanisms; these were, of course, unknown at the time).

The Hodgkin-Huxley equations consist of four coupled ODEs with highly nonlinear terms. For this reason they are quite difficult to understand in an analytic mathematical way. In the next section we explore this model in the elegant way suggested by Fitzhugh. After drawing certain conclusions about the behavior of these equations, we will go on to a much simpler model that captures essential features of the dynamics.

GH'S ANALYSIS OF THE HODGKIN-HUXLEY EQUATIONS

In an elegant paper written in 1960 Fitzhugh set out "to expose to view part of the inner working mechanism of the Hodgkin-Huxley equations." In the year this paper appeared, the three most advanced techniques applied to analysis of nerve conduction models were (1) calculations on a desk calculator (Hodgkin and Huxley's

of the analog computer. Fitzhugh (1960) notes that on the digital computer the solution was very slow, "involving a week or more for a solution, including time for typing instructions to the operating personnel . . ." The analog computer used by Fitzhugh was an electronic device consisting of 40 operational amplifiers, six diode function generators, and five servo multipliers. Being much faster than the digital computers then in use, it permitted greater flexibility in experimenting with the equations, but special precautions were necessary to overcome inaccuracies that would have drastically changed the results for reasons that will become clear presently.

Fitzhugh was the first investigator to apply qualitative phase-plane methods to understanding the Hodgkin-Huxley equations. Since this is a system of four coupled equations (in the variables V , m , n , and h), the phase space resides in R^4 . To make headway in gaining analytic insight, Fitzhugh first considered the variables that change most rapidly, viewing all others as slowly varying parameters of the system. In this way he derived a reduced two-dimensional system that could be viewed as a phase plane. We follow his method here.

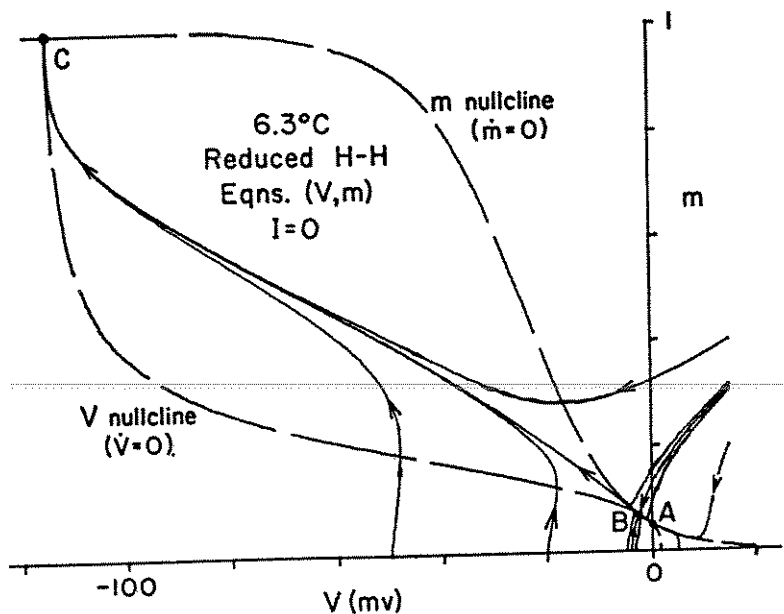
The voltage convention adopted by Fitzhugh $V = v_{out} - v_{in}$ is unfortunately opposite to what subsequently became entrenched in the scientific literature. Thus the first and second quadrants of his phase plane appear reversed relative to the Hodgkin-Huxley model. To avoid possible confusion in conventions we use capital letters when referring to Fitzhugh's analysis.

From the Hodgkin-Huxley equations Fitzhugh noticed that the variables V and m change more rapidly than h and n , at least during certain time intervals. By arbitrarily setting h and n to be constant we can isolate a set of two equations which describe a two-dimensional (V , m) phase plane. Plotting the functional relationships presenting the nullcline equations ($\dot{m} = 0$ and $\dot{V} = 0$) we obtain Figure 8.10. On this figure the three intersections A , B , and C are steady states; A and C are stable nodes, and B is a saddle point.

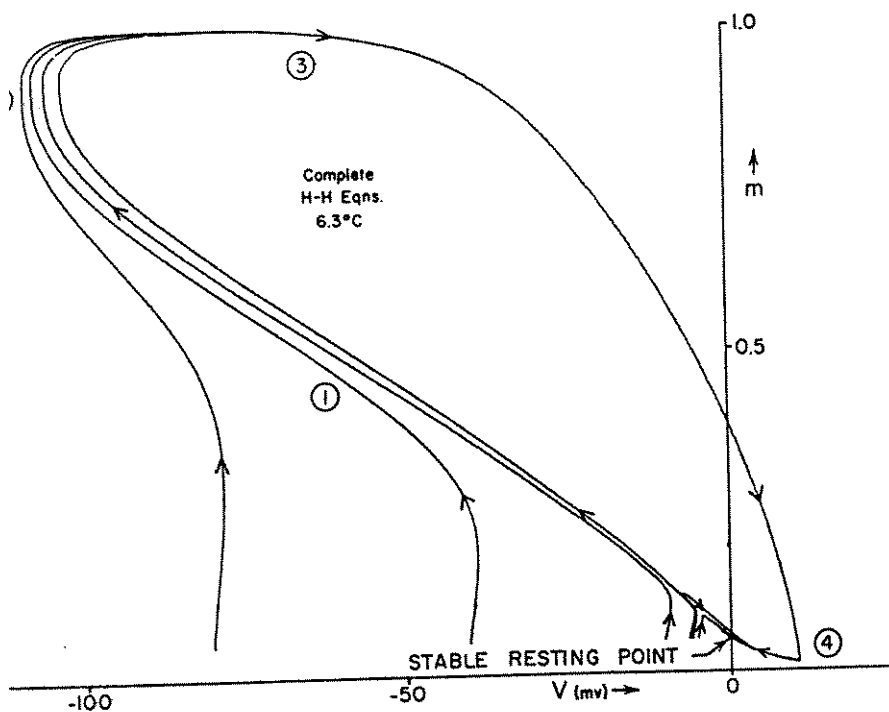
The directions of flow in this plane prescribe the following: A small displacement from the "rest state" at A causes a return to this stable node, but a slightly larger deviation (for example, $m = 0$ and $V = -20$ mV) will lead to a large excursion whose final destination is the attracting point C . Note, however, that the nullclines intersect at very small angles at the points A and B . [See enlarged view, Figure 8.11(a).] Consequently there is great sensitivity to any parameter variations that tend to produce small displacements in these curves. This essentially is the effect of incorporating the modulating influence of the other variables. As some critical parameter changes, a displacement is produced, resulting in the following sequence of dynamic behavior:

- The points A and B approach each other and coalesce.
- These both vanish as the nullclines separate, leaving a single stable steady state at C . When this transition has occurred, any initial state in the Vm plane is drawn towards C .

Adding a third variable, we might next consider the (V , m , h) equations. A heuristic interpretation given by Fitzhugh is to imagine that as a point traces out a trajectory of Figure 8.10(a) the orbits themselves are "wiggling," so that the phase plane is changing with time. By considering the equation for h , Fitzhugh remarks



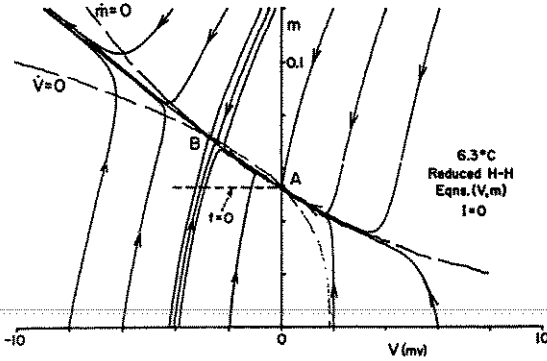
(a)



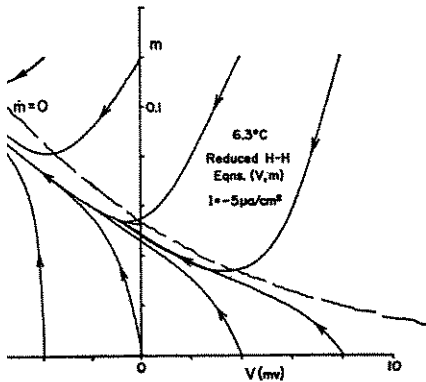
(b)

(a) The reduced phase plane. (b) A complete Hodgkin-Huxley model

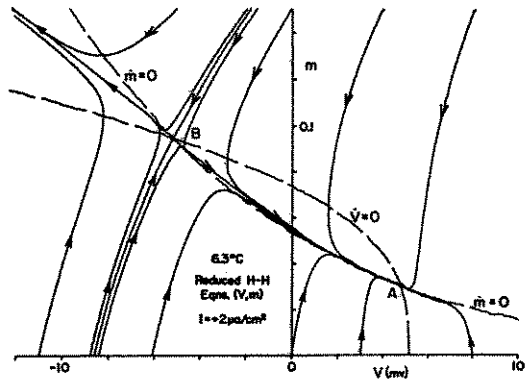
figs. 2 and 9. Reproduced from the J. Gen. Physiol. 1960, vol. 43, pp. 867-896 by copyright permission



(a)



(b)



(c)

Expanded view of the region of the Vm near the steady states B and A. (a) In of stimulating current, A is a stable a saddle point. (b) For super-impulation, A and B coalesce and only C will be a steady state. (c) An

inhibitory stimulus can cause a greater separation of A and B, making it less likely that threshold will be exceeded. [From Fitzhugh (1960), figs. 3, 5, and 6. Reproduced from the J. Gen. Physiol. 1960, vol. 43, pp. 867-896 by copyright permission of the Biophysical Society.]

that as V becomes negative, h decreases, causing an upwards movement in the V nullcline. For small displacements from rest state A this means that B moves to the left, escaping from the moving phase point, which would then return to A. Larger displacements may initially lie to the left of B, in a region that is initially attracted towards C. However, as the geometry shifts, these points may be overtaken by the moving nullclines and forced back to the rest state of A. Fitzhugh gives more details, described in greater subtlety, in a good expository way.

The entire Vmh phase space was reconstructed and represented by a schematic diagram, a projection into the Vm plane. In the complete system there is no saddle point. However, for the variables h and n close to their resting values the system is

entially equivalent to the reduced (V, m) system in which the point B is a saddle point. As seen in Figure 8.10(b) small deviations from the stable resting point do not lead to excitation, but rather to a gradual return to rest. Larger, above-threshold deviations result in a large excursion through phase space, in which V first increases and finally returns with overshoot to the resting state. Such superthreshold trajectories are the phase-space representations of an action potential. The regions marked along these curves with circled numbers correspond to parts of the physiological response which have been called the (1) regenerative, (2) active, (3) absolutely refractory, and (4) relatively refractory phases.

A familiarity with the Hodgkin-Huxley equations underscores the following:

Excitability: Above-threshold initial voltage leads to rapid response with large changes in the state of the system.

Stable oscillations: While not described earlier, the presence of an applied input current represented by an additional term, $I(t)$, on the RHS of equation (9) (e.g. a step function with $I = -10 \mu\text{A cm}^{-2}$) can lead to the formation of a stable limit cycle in the full model (see Fitzhugh, 1961).

Working with these basic characteristics of the Hodgkin-Huxley model led Fitzhugh to propose a simpler model that gives a descriptive portrait of the neural excitation without direct reference to known or conjectured physiological variables. In preparation for an analysis of his much simpler model we take a mathematical detour to become acquainted with several valuable techniques that will prove useful in a number of upcoming results.

POINCARÉ-BENDIXSON THEORY

As previously mentioned, two-dimensional vector fields and thus also two-dimensional phase planes have attributes quite unlike those of their n -dimensional counterparts. One important feature, on which much of the following theory depends, is that a simple closed curve (for example, a circle) subdivides a plane into two disjoint open regions (the "inside" and the "outside"). This result, known as the *Jordan curve theorem* implies (through a chain of reasoning we shall briefly highlight in Appendix 2 for this chapter) that there are restrictions on the trajectories of a smooth two-dimensional phase flow. As discussed in Chapter 5, a trajectory can approach a limiting value only one of the following: (1) a critical point, (2) a periodic orbit, (3) a cycle graph (see Figure 8.12), and (4) infinite xy values. A trajectory contained in a bounded region of the plane can only fall into cases 1 to 3.

The following result is particularly useful for establishing the existence of periodic orbits.

Theorem 1: The Poincaré-Bendixson Theorem

If for $t \geq t_0$ a trajectory is bounded and does not approach any singular point, then it is either a closed periodic orbit or approaches a closed periodic orbit for $t \rightarrow \infty$.

Comment: The theorem still holds if we replace $t \geq t_0$ with $t \leq t_0$ and $t \rightarrow \infty$ with $t \rightarrow -\infty$.

The boxed material outlines properties of a phase plane that are essentially equivalent to the Poincaré-Bendixson theorem and that serve equally well for discovering periodic orbits.

2

Suppose the direction field of the system of equations (1a,b) has the following properties:

1. There is a bounded region D in the plane that contains a single repelling steady state and into which flow enters but from which it does not exit. Then the system (1a,b) possesses a periodic solution (represented by a closed orbit lying entirely inside A or D).
2. There is a bounded annular region A in the plane into which flow enters but from which flow does not exit, and A contains no steady states of equations (1a,b).

It is shown in the appendix that the steady state in part 1 can only be an unstable node or focus.

Two other statements outline the stability properties of periodic solutions.

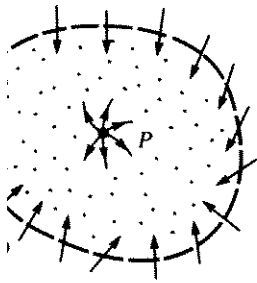
13

1. If either of the regions described in theorem 2 contains only a *single* periodic solution, that solution is a stable limit cycle.
2. If Γ_1 and Γ_2 are *two* periodic orbits such that Γ_2 is in the interior of the region bounded by Γ_1 and no periodic orbits or critical points lie between Γ_1 and Γ_2 , then one of the orbits must be unstable on the side facing the other orbit.

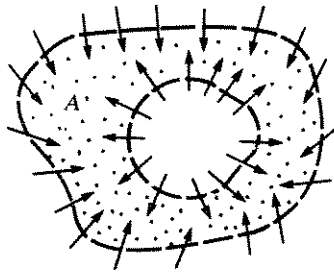
Much of the theoretical work on proving the existence of oscillatory solutions to nonlinear equations such as (1a,b) rests on identifying regions in the phase plane that have the properties described in theorem 2. We now summarize the Poincaré-Bendixson limit-cycle recipe.

ce of Periodic Solutions

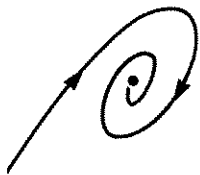
If you can find a region in the xy phase plane containing a single repelling steady state (i.e. unstable node or spiral) and show that the arrows along the boundary of the region never point outwards, you may conclude that there must be at least one closed periodic trajectory inside the region.



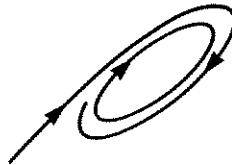
(a)



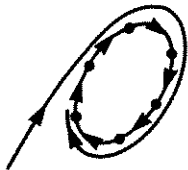
(b)



(c)



(d)



(e)

Poincaré-Bendixson theory
of a limit cycle in two
Flow cannot leave some
as an unstable node or focus.
inside an annular region A in

the xy plane. There are three possible fates of a
bounded semiorbit: (c) approach to a steady state,
(d) approach to a periodic orbit, and (e) approach
to a cycle graph.

An analogous statement corresponding to Figure 8.12(b) can be made. We see several examples of the usefulness of the Poincaré-Bendixson theory in this area.

The two following criteria are sometimes useful in ruling out the presence of a cycle, and for this reason have been called the *negative criteria*:

Bendixson's criterion. Suppose D is a simply connected region of the plane (that is, D is a region without holes). If the expression $\partial F/\partial x + \partial G/\partial y$ is not identically zero (i.e. is not zero for all (x, y) in D) and does not change sign in D , then there are no closed orbits in this region.

Dulac's criterion: Suppose D is a simply connected region in the plane, and suppose there exists a function $B(x, y)$, continuously differentiable on D , such that the expression

$$\frac{\partial(BF)}{\partial x} + \frac{\partial(BG)}{\partial y}$$

is not identically zero and does not change sign in D . Then there are no closed orbits in this region.

The proof of Bendixson's criterion is based on Green's theorem and is accessible to students who have had advanced calculus (see appendix to this chapter). Dulac's criterion is an extension that results by substituting BF for F and BG for G in the proof of Bendixson's criterion. For an interesting example of the utility of Dulac's criterion, consider a two-species competition model with carrying capacity κ_i :

$$\frac{dx}{dt} = r_1x \frac{\kappa_1 - x - \beta_{12}y}{\kappa_1} \tag{14a}$$

$$\frac{dy}{dt} = r_2y \frac{\kappa_2 - y - \beta_{21}x}{\kappa_2} \tag{14b}$$

For eliminating limit cycles, Bendixson's criterion fails, but Dulac's criterion succeeds by choosing $B(x, y) = 1/xy$. (See problem 5.) Based on Bendixson's criterion, the following result is readily established.

of Bendixson's Criterion:

If equations (1a,b) are linear in x and y , then the only possible oscillations are the neutrally stable ones. (Limit cycles can only be obtained with nonlinear equations.)

To understand why this is true, consider the system (1a,b) where $f(x, y) = ax + by$, $G(x, y) = cx + dy$; then $F_x + G_y = a + d$. This is a constant and has a fixed sign. Thus the criterion is only satisfied trivially if $a + d = 0$ in which case the equations would be $dx/dt = by$ and $dy/dt = dx$. Such equations have neutral cycles (not limit cycles), provided b and d have opposite signs.

Comments: Bendixson's negative criterion does not say what happens if the expression $\partial F/\partial x + \partial G/\partial y$ does change sign. (No conclusions can then be drawn about the existence of limit cycles.) In other words, the theorem gives a necessary but *not* a sufficient condition to test.

CASE OF THE CUBIC NULLCLINES

As one application of the Poincaré-Bendixson theorem we examine a rather classical phase-plane geometry that almost invariably leads to the properties of oscillation or excitability. We first discuss a prototype in which one of the nullclines is a simple cubic curve [equation (16)]. As the qualitative analysis will illustrate, this configuration creates the geometry to which the Poincaré-Bendixson theorem applies. An extension to more general S-shaped nullclines will easily follow.

consider the system of equations

$$\dot{u} = v - G(u), \tag{15a}$$

$$\dot{v} = -u, \tag{15b}$$

for our prototype we take $G(u)$ to be

$$G(u) = \frac{u^3}{3} - u. \tag{16}$$

all postpone a discussion of the motivation underlying these equations and concentrate first on understanding their behavior. One important feature of the function exploited presently is that

$$G(u) = -G(-u),$$

G is an *odd* function. Nullclines of this system are the loci of points

$$v = G(u) \quad (\text{the } u \text{ nullcline}), \tag{17}$$

$$u = 0 \quad (\text{the } v \text{ nullcline}). \tag{18}$$

The term *cubic nullcline* now becomes somewhat more transparent. The shape of the loci given by equation (17) is that of a cubic curve, symmetric about the v axis. The two humps to the left and right of the origin also play an important role in determining the properties of the system. (For this reason the function $G(u) = u^3$ would not be satisfactory; see problem 10 and Figure 8.13.)

Now consider the pattern of flow along these nullclines. The following points can be deduced from the equations:

The direction must be “vertical” on the u nullcline and “horizontal” on the v nullcline (since $\dot{u} = 0$ or $\dot{v} = 0$, respectively).

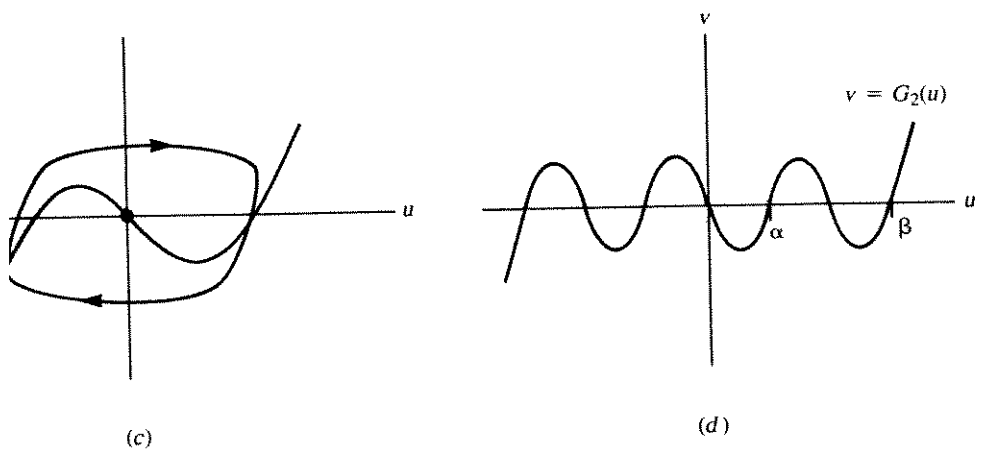
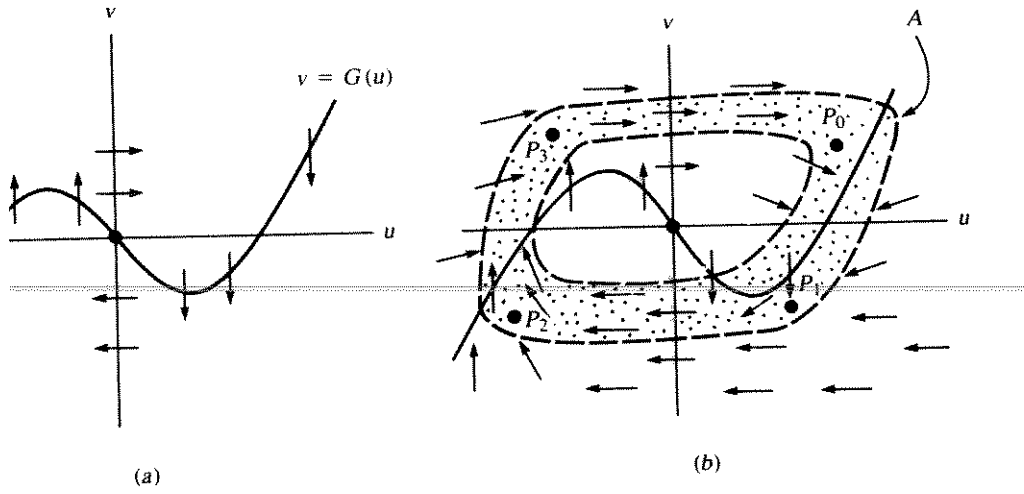
Whenever u is positive, v decreases.

On the v nullcline, u is zero so that $G(u)$ is also zero. Thus by equation (15a) $\dot{u} = v$, and u will increase when v is positive and decrease when v is negative.

These conclusions are depicted in Figure 8.13(a).

Now consider a trajectory emanating from some arbitrary point $P_0(x_0, y_0)$ in the annular region in Figure 8.13(b). The flow in proximity to the u nullcline will cross it and towards decreasing u values. After arriving at P_1 , the flow drifts vertically across the v axis and over to the left branch of the cubic curve (P_2). A current in the positive v direction conveys the point to P_3 and then back to the top of the hump and into the positive quadrant. From the construction in the diagram it is further evident that the direction of flow is everywhere *into* or *parallel to* the boundary of the annular region, indicating that once a trajectory has entered the region, it is forever trapped. There are no steady-state points in A , and A is bounded. By the Poincaré-Bendixson theorem we can conclude that there is a limit cycle trajectory inside this region.

Furthermore, it is possible to shrink the thickness of A to an arbitrarily fine region and draw similar conclusions. In particular, this means that we can dismiss the



(a) Flow along cubic nullclines described by (15) and (16); (b) an annular region of flow in the uv plane; (c) a limit cycle

oscillation contained in the region A ; (d) more general shapes of the function G that lead to similar results.

possibility that there is more than one limit cycle in the dynamical system. (See Problem 10.)

We have chosen a particular example in which the form of the equations leads to certain specific features: (steady state at $(0, 0)$, flow symmetric with respect to the origin, and one nullcline along the y axis). These features can be changed somewhat without losing the main dynamic features of the system. More generally, a broader class known as the *Lienard equations* exhibit similar behavior. Sometimes written as the following single equation,

$$\frac{d^2u}{dt^2} + g(u) \frac{du}{dt} + u = 0, \tag{19}$$

be shown to be equivalent to the system of (15a,b), where

$$G(u) = \int_0^u g(s) ds. \tag{20}$$

the following properties of $G(u)$ lead to a generalized cubic that results in essentially identical conditions:

$G(u) = -G(-u)$ (thus $G(u)$ is an odd function).
 $G(u) \rightarrow \infty$ for $u \rightarrow \infty$ (the right and left branches of G extend to $+\infty$ and $-\infty$)
 and for some positive β , $G(u) > 0$ and $dG/du > 0$ whenever $u > \beta$; (G is eventually positive and monotonically increasing).
 For some positive α , $G(\alpha) = 0$ and $G(u) < 0$ whenever $u < \alpha$. (G is negative for small positive u values).

Condition 1 means that all trajectories will be symmetric about the origin. Condition 2 is necessary to cause the flow to be trapped or confined to the given annulus. Condition 3 means that the steady state at $(0, 0)$ is unstable. (Details are integrated in problem 11.) An example of a "bumpy" function satisfying these conditions is shown in Figure 8.13(d). It can be rigorously established (with reasoning similar to that used earlier) that such conditions guarantee that the system of equations (15) (or the single equation 19) admits a nontrivial periodic solution, that is, a cycle. In the particular case where $\alpha = \beta$, as in the example we have analyzed, there is indeed a single periodic orbit that is asymptotically stable. Rigorous proof and further details may be found in Hale (1980), (p. 57-63).

The example used as a prototype in this section is called the *Van der Pol oscillator*, sometimes written in the form

$$\ddot{u} - k(1 - u^2)\dot{u} + u = 0 \quad (k > 0). \tag{21}$$

(problem 12.) Van der Pol first used it in 1927 to represent an electric circuit containing a nonlinear element (a triode valve whose resistance depends on the applied current). Even then, van der Pol realized the parallel between this circuit and biological oscillations such as the heart beat. For large values of the constant k the corresponding system of equations

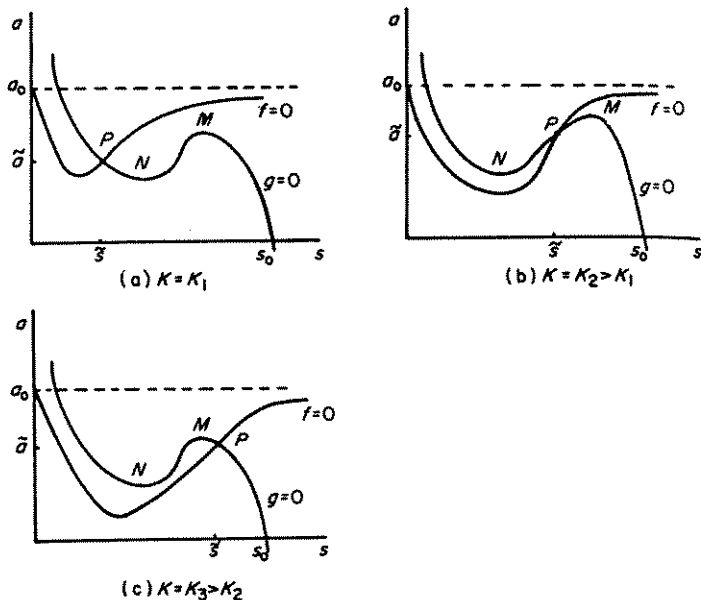
$$\epsilon \dot{u} = v - G(u), \tag{22a}$$

$$\dot{v} = -u\epsilon, \tag{22b}$$

admits a small parameter $\epsilon = 1/k$. (Recall that this can be exploited in calculating approximate solutions using techniques of asymptotic expansions. See problem 12 for a taste of the idea.) The solutions to this small-parameter system are called *relaxation oscillations* for the following reasons: as long as v is close to $G(u)$ (that is, in the vicinity of the cubic curve), \dot{u} and \dot{v} both change rather slowly. When the trajectory

departs from this curve, $\dot{u} = [v - G(u)]/\epsilon$ is quite large. The horizontal progression across from P_1 to P_2 is thus rapid. A plot of $u(t)$ reveals a succession of time intervals in which u changes slowly followed by ones in which it changes more rapidly.

Models related to van der Pol's oscillator have been important in many physical settings and, as we shall see, have also been valuable in describing oscillating biological systems. (A example of an application to the heart-beat cycle is discussed in Jones and Sleeman, 1983.) More generally, the idea underlying s -shaped nullclines has been exploited in a variety of models for excitable and oscillatory phenomena. Figures 8.14 to 8.17 are a sampling drawn from the literature, and Section 8.5 deals in greater detail with one particular application in the study of neural signals.



Several regimes of behavior in a model inhibition with S-shaped nullclines. s is substrate and a is cosubstrate. Their dynamics are represented by the equations

$$\dot{s} = g(s, a), \quad \frac{da}{dt} = f(s, a)$$

$$g(s, a) = s_0 - s - \frac{\rho sa}{1 + s + Ks^2},$$

$$f(s, a) = \alpha(a_0 - a) - \frac{\rho sa}{1 + s + Ks^2}.$$

K is the inhibition parameter, α , ρ , a_0 and s_0 are constants (see details in the original reference.) M and N represent the maximum and minimum points along the nullcline $g = 0$, and P is the steady state. The transition a) \rightarrow b) \rightarrow c) is for decreasing K -values. [From Murray (1981), fig. 2, p. 168. J. Theor. Biol., 88, 161-199. Reprinted by permission of Academic Press Inc. (London)]

field and cubic
or respiration in a
nutrient x and oxygen
by the equations

$$\frac{xy}{1 + qx^2} = F(x, y),$$

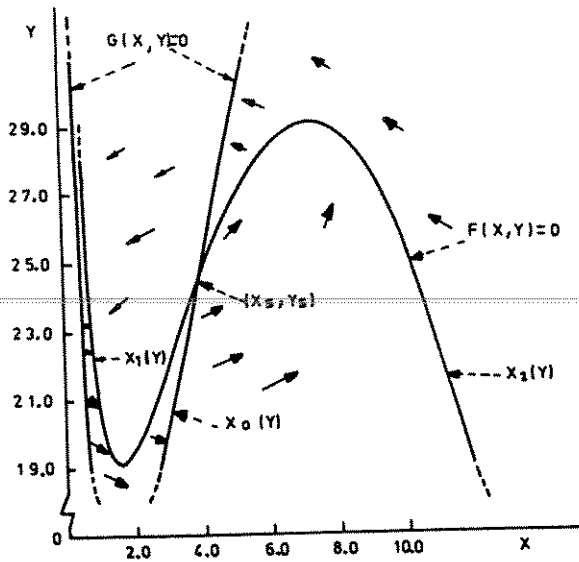
$$\frac{xy}{1 + qx^2} = G(x, y).$$

values for stable oscillations are

$$q = 0.5.$$

Parde (1979). Fig. 3.

..., 8, 147-157, by
Verlag.]



limit-cycle oscillations, and (b)
threshold perturbation, in a
system derived from equations for a
system devised by Goldbeter
the original equations are

(intracellular ATP),

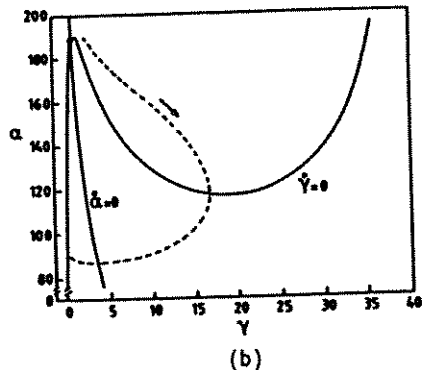
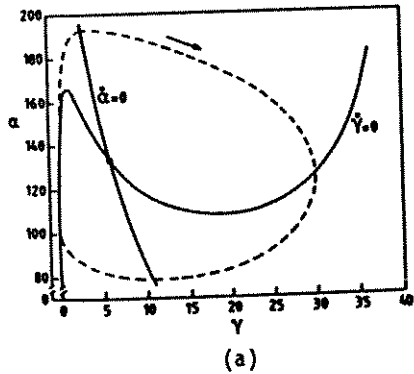
β (intracellular CAMP),

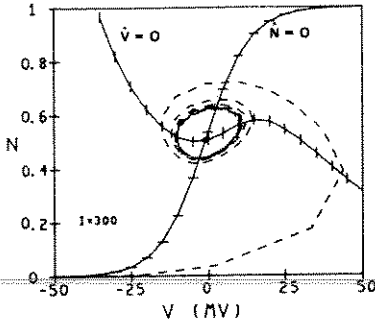
(extracellular CAMP),

dimensionless metabolic

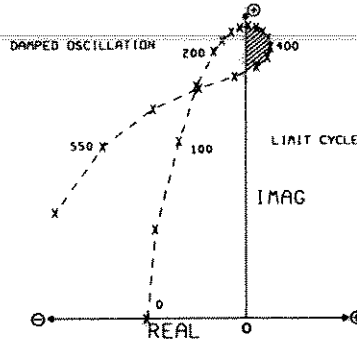
$\frac{1 + \gamma)^2}{1 + \gamma)^2}$ (allosteric kinetics
of adenylate cyclase)

term depicting enzyme —
s. See Segel (1984) for a
and definitions of parameters.
and Martiel (1983). A critical
model for relay and
AMP in dictyostelium cells, in
and other Fields of Application
Symposium, vol. 49, pp 173-178.
with the author's permission.]





(a)



(b)

7 (a) S-shaped nullclines in a model for oscillations in the barnacle giant muscle. v_n is a limit cycle in a reduced V , N = voltage and N = fraction of open K^+ channels. V satisfies an equation like (9), and N is

(b) The eigenvalues of the linearized system change as the current is increased and cross the imaginary axis twice. [From Morris and Lecar (1981), figs. 7 and 8. Reproduced from the Biophysical Journal (1981) vol 35, 193–213, by copyright permission of the Biophysical Society.]

$$\frac{dN}{dt} = \lambda_N(V)(N_\infty(V) - N),$$

$$N_\infty = \frac{1}{2} \left(1 + \tanh \frac{v - v_3}{v_4} \right).$$

itions

A system of equations (1a,b) in which one of the nullclines $F(x, y) = 0$ or $G(x, y) = 0$ is an S-shaped curve can give rise to oscillations provided the steady state on this curve is unstable.

When the steady state is stable, the system may exhibit a somewhat different behavior called excitability. We discuss this property further in Section 8.5.

FITZHUGH-NAGUMO MODEL FOR NEURAL IMPULSES

In section 8.2 we followed an analysis of the Hodgkin-Huxley model published by Fitzhugh in the biophysical literature in 1960. The elegance of applying phase-plane methods and reduced systems of equations to this rather complicated problem should not be underestimated. (Similar ideas are used in more recent examples; see Morris and Lecar, 1981.)

Using such analysis, Fitzhugh was able to explain the occurrence of thresholds in the Hodgkin-Huxley model of neural excitation. The analysis was, however, less effective in demonstrating causes of *repetitive impulses* (a sequence of action potentials in the neuron) because here the interactions of all four variables — V , m , h , and n — were important [see equations (9) to (12).] A greater reliance on numerical, rather than analytic techniques was thus necessary.

In a succeeding paper published in 1961, Fitzhugh proposed to demonstrate that the Hodgkin-Huxley model belongs to a more general class of systems that exhibit the properties of excitability and oscillations. As a fundamental prototype, the van der Pol oscillator was an example of this class, and Fitzhugh therefore used it (with suitable modification). A similar approach was developed independently by Nagumo et al. (1962) so the following model has subsequently been called the Fitzhugh-Nagumo equations.

To avoid misunderstanding, it should be emphasized that the main purpose of this model is not to portray accurately quantitative properties of impulses in the axon. Indeed, the variables in the equations have somewhat imprecise meanings, and their relationships do not correspond to exact physiological facts or conjectures. Rather, the system is meant as a simpler paradigm in which one can exhibit the sorts of interactions between variables that lead to properties such as excitability and oscillations (repetitive impulses).

Fitzhugh proposed the following equations:

$$\frac{dx}{dt} = c \left[y + x - \frac{x^3}{3} + z(t) \right], \quad (23a)$$

$$\frac{dy}{dt} = - \frac{x - a + by}{c}. \quad (23b)$$

In these equations the variable x represents the excitability of the system and could be identified with voltage (membrane potential in the axon); y is a recovery variable, representing combined forces that tend to return the state of the axonal membrane to rest. Finally, $z(t)$ is the applied stimulus that leads to excitation (such as input current). In typical physiological situations, such stimuli might be impulses, step functions, or rectangular pulses. It is thus of interest to explore how equations (23a,b) behave when various functions $z(t)$ are used as inputs. Before addressing this question we first take $z = 0$ and analyze the behavior of the system in the xy phase plane.

In order to obtain suitable behavior, Fitzhugh made the following assumptions about the constants a , b , and c :

$$1 - \frac{2b}{3} < a < 1, \quad 0 < b < 1, \quad b < c^2, \quad (24)$$

Inspection reveals that when $z = 0$, nullclines of equations (23a,b) are given by the following loci:

$$y = \frac{x^3}{3} - x \quad (\dot{x} = 0, \text{ the } x \text{ nullcline}), \quad (25)$$

$$y = \frac{a - x}{b} \quad (\dot{y} = 0, \text{ the } y \text{ nullcline}). \quad (26)$$

The humps on the cubic curve are located at $x = \pm 1$.

We shall not explicitly solve for the steady state of this system, which satisfies the cubic equation

$$\frac{x^3}{3} + x\left(\frac{1}{b} - 1\right) = \frac{a}{b}. \quad (27)$$

However, the conditions given by equation (24) on the parameters guarantee that there will be a *single* (real) steady-state value (\bar{x}, \bar{y}) located just beyond the negative hump on the cubic x nullcline, at its intersection with the skewed y nullcline, as shown in Figure 8.18.

Calculating the Jacobian of equations (23) leads to

$$\mathbf{J} = \begin{pmatrix} (1 - \bar{x}^2)c & c \\ \frac{-1}{c} & \frac{-b}{c} \end{pmatrix} \quad (28)$$

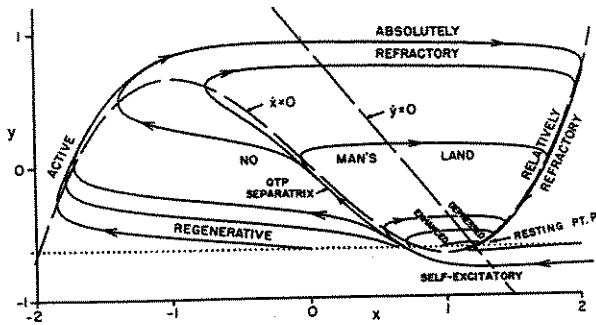
(problem g). Thus, by writing the characteristic equation in terms of \bar{x} , we obtain the quadratic equation

$$\lambda^2 + \left[\frac{b}{c} - (1 - \bar{x}^2)c \right] \lambda + [1 - (1 - \bar{x}^2)b] = 0. \quad (29)$$

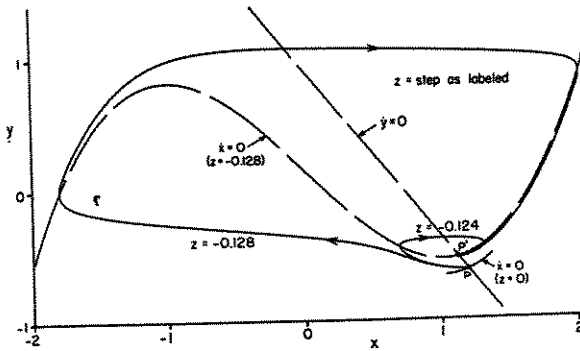
The steady state will therefore be stable provided that

$$-\left[\frac{b}{c} - (1 - \bar{x}^2)c \right] < 0, \quad (30a)$$

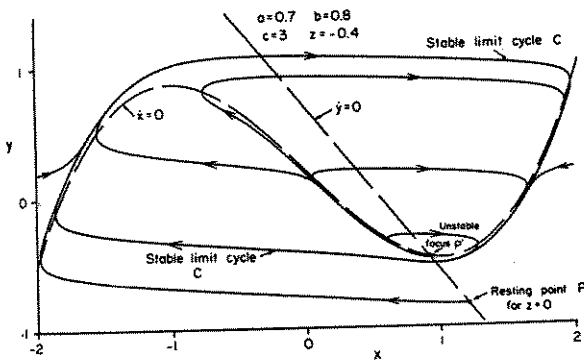
$$1 - (1 - \bar{x}^2)b > 0. \quad (30b)$$



(a)



(b)



(c)

gh's model [equations 23a,b] phase-plane behavior shown in text for an interpretation of x , y and z . Resting point corresponds to the resting potential. (b) In the presence of a step input ($z = -0.128$) the system behaves in a manner analogous to a single action

potential. (c) For a step input of stronger current, an infinite train of impulses (repetitive action potentials) are generated. [From Fitzhugh (1961), figs. 1, 3, and 5. Reproduced from the Biophysical Journal, 1961, vol 1, pp 445-466, by copyright permission of the Biophysical Society.]

Continuous Processes and Ordinary Differential Equations

Note that these conclusions are not affected if z in equation (23a) is nonzero. Since $b < 1$ and $b < c^2$, it may be shown (problem g) that the steady state is stable for all values of \bar{x} that are not in the range

$$-\gamma \leq \bar{x} \leq \gamma, \quad (31)$$

where $\gamma = (1 - b/c^2)^{1/2}$ is a positive number whose magnitude is smaller than 1. The geometry shown in Figure 8.18 tells us that if the y nullcline were to intersect the cubic x nullcline somewhere on the middle branch between the two humps, the steady state would be unstable.

We next consider the behavior of the *stimulated* neuron, described by equations (23a,b) with a nonzero stimulating current $z(t)$. A particularly simple set of stimuli might consist of the following:

1. A step function $z = 0$ for $t < 0$; $z = i_0$ for $t \geq 0$.
2. A pulse ($z = i_0$ for $0 \leq t \leq t_0$; $z = 0$ otherwise).
3. A constant current $z = i_0$.

For as long as $z = i_0$, the configuration of the x nullcline is given by the equation

$$y = \frac{x^3}{3} - x + i_0. \quad (32)$$

This cubic curve has been shifted in the positive y direction if i_0 is positive and in the opposite direction if i_0 is negative. Let S^* represent the intersection of (32) with the y nullcline, S^0 the intersection of (25) with the y nullcline, and S the instantaneous state of the system. Thus S^* and S^0 are the steady states of the stimulated and unstimulated system, respectively and $S = (x(t), y(t))$.

At the instant a stimulus is applied, $S = S^0$ is no longer a rest state, since the steady state has shifted to S^* . This means that S will change, tracing out some trajectory in the xy plane. The following possibilities arise:

1. If i_0 is very small, S^* will be close to S^0 , on the region of the cubic curve for which steady states are stable and $S = (x(t), y(t))$ will be attracted to S^* without undergoing a large displacement.
2. If i_0 is somewhat larger, S^* may still be in the stable regime, but a more abrupt dynamics could ensue: in particular, if S falls beyond the separatrix shown in Figure 8.18(a), the state of the system will undergo a large excursion in the xy plane before settling into the attracting steady state S^* .

Such cases represent a single action-potential response that occurs for superthreshold stimuli. (See Figure 8.3.) This type of behavior, in which a steady state is attained only after a long detour in phase space, is typical of *excitable systems*. As we have seen, it is also a property intimately associated with systems in which one or both the nullclines have the S shape (also referred to sometimes as N shape or z shape similar to that of the cubic curve).

3. For yet larger i_0 , S^* will fall into the middle branch of the cubic curve so that it is no longer stable. In this case the situation discussed in Section 8.5 occurs and a stable, closed, periodic trajectory is created. All points, and in particular

S , will undergo cyclic dynamics, approaching ever closer to the stable limit cycle. This behavior corresponds to *repetitive firing* of the axon, which results when a step stimulus of sufficiently high intensity is applied.

In all of these cases, when the applied stimulus is removed (at $z = 0$), S^0 becomes an attracting rest state once more; the repetitive firing ceases, and the excited site eventually returns to rest.

With a few masterful strokes, Fitzhugh has painted a *caricature* of the behavior of neural excitation. His model is not meant to accurately portray the physiological mechanisms operating inside the axonal membrane. Rather, it is a behavioral radigm, phrased in terms of equations that are mathematically tractable. As such it has played an important role in leading to an understanding of the nature of excitable systems and in studying more complicated models of the action potential that include the effect of spatial propagation in the native (nonclamped) axon.

7 BIFURCATION

A further diagnostic tool that can help in establishing the existence of a limit-cycle trajectory is the *Hopf bifurcation theorem*. It is quoted widely, applied in numerous contexts, and for this reason merits discussion.

Subject to certain restrictions, this theorem predicts the appearance of a limit cycle about any steady state that undergoes a transition from *a stable to an unstable focus* as some parameter is varied. The result is local in the following sense: (1) The theorem only holds for parameter values close to the *bifurcation value* (the value at which the just-mentioned transition occurs). (2) The predicted limit cycle is close to the steady state (has a small diameter). (The Hopf bifurcation does not specify what happens as the *bifurcation parameter* is further varied beyond the immediate vicinity of its critical bifurcation value.)

In the following box the theorem is stated for the case $n = 2$. A key requirement corresponding to our informal description is that the given steady state be associated with *complex* eigenvalues whose real part changes sign (from $-$ to $+$). In popular phrasing, such eigenvalues are said to “cross the real axis.” To recall the connection between complex eigenvalues and oscillatory trajectories, consider the discussion in Section 5.7 (and in particular, Figure 5.12 of Chapter 5).

Advanced mathematical statements of this theorem and its applications can be found in Marsden and McCracken (1976). Odell (1980) and Rapp (1979) give good informal descriptions of this result that are suitable for nonmathematical readers.

One of the attractive features of the Hopf bifurcation theorem is that it applies to larger systems of equations, again subject to certain restrictions. This makes it somewhat more applicable than the Poincaré-Bendixson theorem, which holds only for the case $n = 2$.